Journal of Marine Systems, 2 (1991) 81–95
Elsevier Science Publishers B.V., Amsterdam

The transport of CO_2 into Arctic and Antarctic Seas: Similarities and differences in the driving processes

Leif G. Anderson [a] and E. Peter Jones [b]

[a] *Department of Analytical and Marine Chemistry, University of Goteborg and Chalmers University of Technology, S-412 96 Göteborg, Sweden*

[b] *Department of Fisheries and Oceans, Bedford Institute of Oceanography, P.O. Box 1006, Dartmouth, N.S. B2Y 4A2, Canada*

Received September 3, 1990; revised version accepted January 29, 1991

ABSTRACT

Anderson, L.G. and Jones, E.P., 1991. The transport of CO_2 into Arctic and Antarctic Seas: Similarities and differences in the driving processes. J. Mar. Syst., 2: 81–95.

The transport of CO_2 from the atmosphere to the surface water of the ocean is driven by the difference in partial pressure of CO_2 at the air–sea interface. Since the atmospheric partial pressure of CO_2 is nearly constant over periods of the order of exchange times, changing conditions of the surface of the ocean dominate the exchange process. In polar regions, the partial pressure of CO_2 in the ocean is decreased mainly by two processes, a decrease in temperature and biological productivity. Both of these take place in the Arctic and Antarctic.

In the Arctic, the vertical transport of cooled surface water by deep convection mainly takes place in the Greenland Sea and penetrates to a very large depth, while in the Antarctic the deep convection does not reach the same depths, at least not as frequently. Biological production is significant for the vertical transport of carbon in both the Arctic and Antarctic; however, in the Arctic the production is mainly over the large shelves, while in the Antarctic it takes place mostly over the deep ocean.

In addition to cooling, surface water can also increase its density by salt addition from ice formation. When this happens over the shelves, high density shelf bottom waters are formed that might be enriched in total carbonate due to decay of organic matter at the sediment surface. These high density bottom waters flow towards the deep ocean, mixing with surrounding waters during transit and ending up at a matching density surface. This process seems to be quantitatively more important in the Arctic than in the Antarctic.

Total alkalinity, total carbonate, calcium, oxygen, salinity and temperature data from several expeditions in the Arctic and the SWEDARP 88/89 expedition in the Antarctic are used in this discussion.

Introduction

The polar seas of both hemispheres, the waters surrounding Antarctica and in the Arctic Ocean, are similar in several respects yet quite different in others. They are both partly covered by sea ice whose extent varies with season. A main difference is that in Antarctica the areas which are ice free in the summer and ice covered in the winter are mainly over deep water, while in the Arctic these areas are mainly over the continental shelves (Fig. 1). This reflects a major difference in topography: in Antarctica, the ocean surrounds the continent, while in the Arctic, the ocean is surrounded by continents. Furthermore, in Antarctica there are large ice shelves which flow from the continent into the surrounding seas. These differences also makes the processes involved in the transport of atmospheric gases (e.g., CO_2) into the sea different.

The exchange of gases between the atmosphere and seawater in contact with the atmosphere depends on the partial pressures of the gases in the two mediums. For CO_2, the partial pressure in

0924-7963/91/$03.50

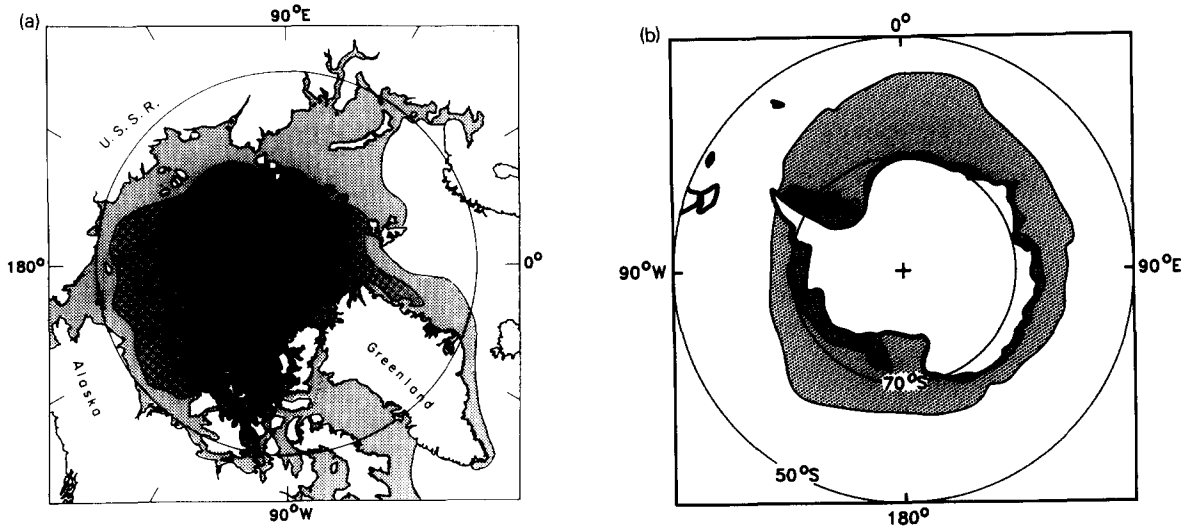

Fig. 1. Map of the (a) Arctic and (b) Antarctic showing the typical maximum and minimum ice cover.

seawater is set by the concentration of total carbonate (C_t) and total alkalinity (A_t), which are defined as

$$C_t = [CO_3^{2-}] + [HCO_3^-] + [H_2CO_3] + [CO_2]$$

and

$$A_t = [HCO_3^-] + 2[CO_3^{2-}] + [B(OH)_4^-] + [HPO_4^{2-}] + 2[PO_4^{3-}] + [SiO(OH)_3^-] + [OH^-] - [H^+] - [HSO_4^-] - [HF^-] - [H_3PO_4]$$

The solubility of CO_2 in seawater increases with decreasing temperature (Weiss, 1974). With a constant A_t and 100% CO_2 saturation, the relation between C_t and temperature in seawater varies for different atmospheric pressures according to Fig. 2 (after Dyrssen and Wedborg, 1982). It is obvious from this figure that all surface waters today have a higher C_t compared to preindustrial times, providing, as is likely, that biological processes have remained the same over this time interval.

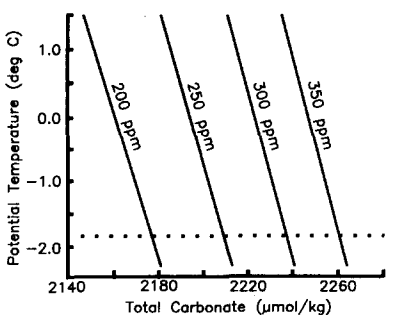

Fig. 2. Total carbonate as a function of potential temperature for seawater of constant total alkalinity (2387 μmol/kg) in equilibrium with atmospheres of different pCO_2.

A_t and C_t are affected by different biological processes to different degrees. The two dominating processes are the production-decay of organic matter and the precipitation-dissolution of metal carbonate, mainly calcium and magnesium carbonate. Furthermore, C_t is also affected by CO_2 exchange with the atmosphere, but this does not change A_t as can be seen from the definition.

The formation of organic matter can be represented by the following simple model, with the model substance including carbohydrates, lipids, peptides, phosphate esters and trace metals (Dyrssen, 1977).

$$(x+y+33)CO_2 + (x+y+16)H_2O + 16NO_3 + H_2PO_4 + 15H + M \rightarrow (CH_2O)_x(CH_2)_y(CH_2NHCO)_{16}C(MHPO_4) + (2x+3y+114)/2O_2$$

The change in A_t due to this reaction is +15 and in C_t is $-(x+y+33)$. The sum of $x+y+33$ was reported to be 106 by Redfield et al. (1963) and to be 103 ± 14 by Takahashi et al. (1985). The oxygen produced during primary production,

$(2x + 3y + 114)/2$, was reported by the same authors to be 138 and 172 with respect to each phosphate consumed.

The reaction for formation of metal carbonate, here illustrated by calcium, is

$$Ca^{2+} + 2HCO_3^- \rightarrow CaCO_3(s) + CaCO_3(s) + CO_2 + H_2O.$$

The ratio of the shifts of A_t to C_t is 2 if the CO_2 stays in the water and 1 if the CO_2 is ventilated to the atmosphere. The decay of organic matter and dissolution of metal carbonate will proceed in the direction opposite to the above reactions.

The concentration in the ocean is typically about 2350 μmol/kg (micro mole acid consumed) for A_t and about 2200 μmol/kg for C_t. The natural variation is normally around 10–20 μmol/kg with the maximum being up to 100 μmol/kg. With high precision determinations of A_t, C_t and oxygen, it is possible to correct for decay of organic matter and dissolution of metal carbonate to get the preformed concentrations of A_t and C_t. With this knowledge of the preformed concentrations, we can determine the degree of CO_2 saturation when a water parcel left the surface.

In this article we will summarize today's knowledge of the input of atmospheric CO_2 into the Polar Seas. We will describe the processes that are responsible for the transport and compare them for the two polar oceans. Furthermore we will make some quantitative estimates of the CO_2 inputs.

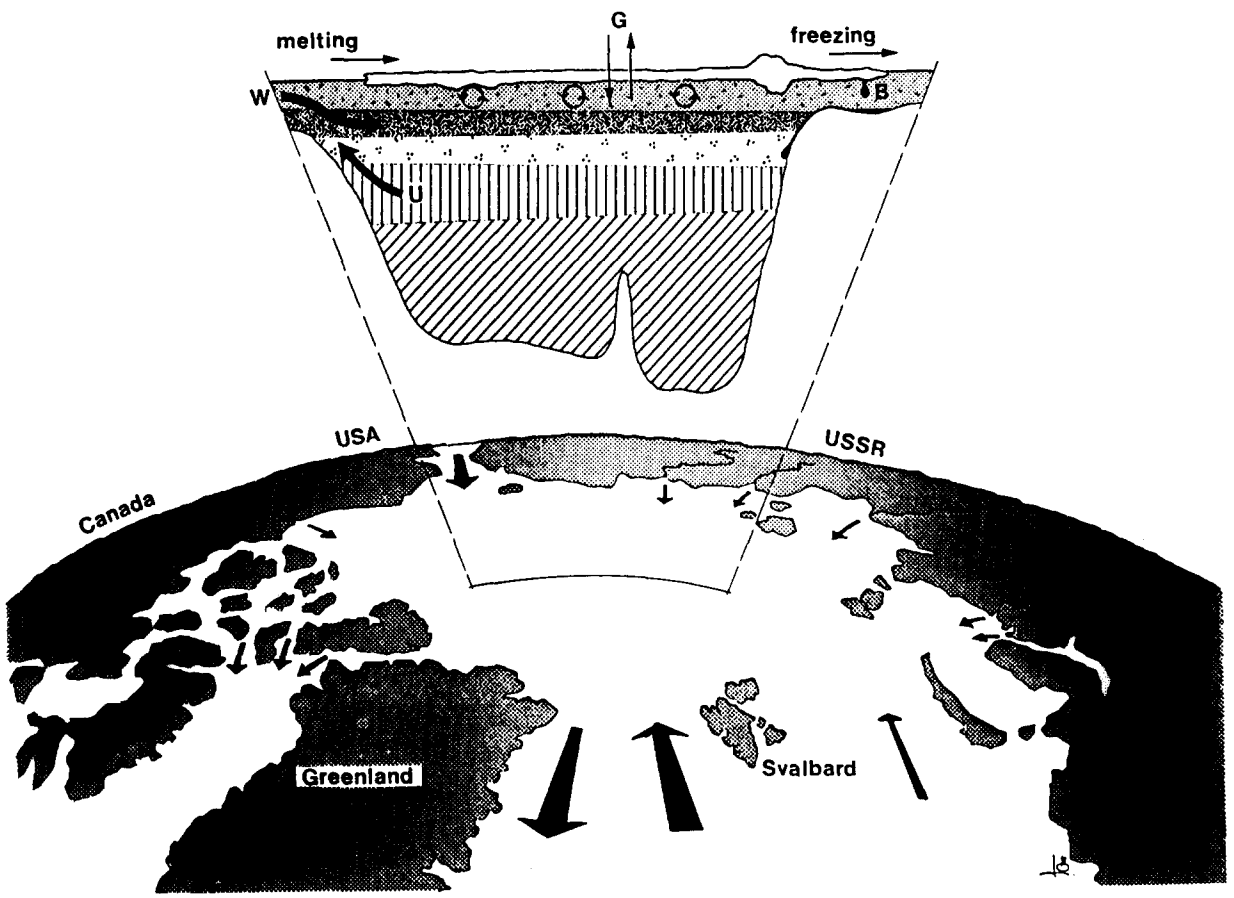

Fig. 3. The Arctic Ocean with inflows and outflows. The schematic depth section illustrates the different main water masses. *G* denotes gas transfer; *W*, inflow of water through Bering Strait; *B*, brine drainage; *U*, upwelling of Atlantic layer water. (From Anderson and Dyrssen, 1989.)

The Arctic Ocean

The Arctic Ocean consists of four deep basins surrounded by large shallow shelves, with connections to other oceans through Bering Strait, the Canadian Archipelago and Fram Strait. Fram Strait provides the only deep connection with other oceans and is thus the only place where deep water exchange can take place. Water enters the Arctic Ocean through Bering Strait, Fram Strait and Barents Sea and leaves through the Canadian Archipelago and Fram Strait. There is also a significant river run-off, about 0.1×10^6 m^3s^{-1} (e.g. Aagaard and Carmack, 1989), mainly from the Siberian rivers. An illustration of the water transports into and out of the Arctic Ocean as well as the vertical water mass distribution is shown in Fig. 3.

In the Arctic Ocean we find different water masses at various depths. These water masses are thought to be rather homogeneous throughout much of the region. The various water masses result from the salinity variations in the different source waters (Atlantic and Pacific) and from modifications resulting from the freezing–melting processes taking place within the Arctic Ocean proper. At the surface is the surface mixed layer with a constant temperature of close to freezing and a salinity of 31–32. Below this layer, starting at 50 to 70 m, the salinity increase dramatically while the temperature remains quite constant at temperatures close to freezing. This water mass, the upper halocline, is centered around about 130 m. Going deeper, the temperature increases and the salinity continues to increase. Before we reach the temperature maximum (the signature of the Atlantic layer) there is a distinct change in slope of the T–S curve (Fig. 4) at a salinity of about 34.3, indicating the center of the lower halocline. Below the Atlantic layer is the deep water which can be divided into several components (Aagaard et al., 1985) with the signature of the bottom water varying between the different basins.

Deep water formation

Deep water is not formed by deep convection in central regions of the Arctic Ocean as the stratification is too strong. However, deep water is formed by convection in the Greenland See just south of Fram Strait (e.g., Rudels, 1986). The deep water thus formed is modified by mixing and flows north through Fram Strait into the Arctic Ocean (Smethie et al., 1988) where high salinity shelf water is added, increasing the salinity to values higher than any water south of Fram Strait (Swift et al., 1983). A schematic illustration of the deep water formation in the Fram Strait region and the mixing of the different water masses is shown in Fig. 5.

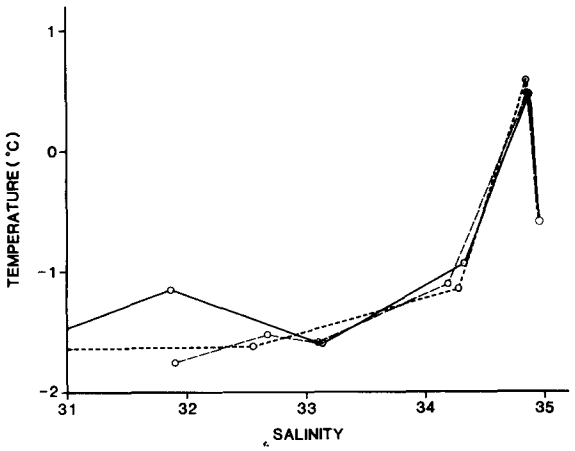

Fig. 4. Potential temperature versus salinity in the central Arctic Ocean. The data are from ——— line (Kinney et al., 1970), LOREX - - - - - line (Moore et al., 1983) and CESAR — — — line (Jones and Anderson, 1986). (From Anderson and Dyrssen, 1989.)

High density water is formed in the Arctic Ocean by brine drainage during sea ice formation and ageing. As most of the ice is formed over the shallow shelves, the brine will result in a cold, high salinity pool of water on the shelf bottom (Aagaard et al., 1981; Melling and Lewis, 1982; Midttun, 1985). This pool can, if the topographic conditions are right, drain along the shelf bottom and down the shelf break towards the deep interior, entraining surrounding water as it flows (e.g., Quadfasel et al., 1988). It will interleave at a depth that matches its density. Most of this shelf-produced cold, high salinity water ends up in the upper halocline (e.g. Björk, 1989). This is why the salinity in the upper halocline increases relative to the surface mixed layer while the temperature stays close to freezing.

Data

The carbonate data to study the input through deep convection were collected during the YMER-80, the Hudson-82 and the MIZEX-84 expeditions, all in the Fram Strait region. The YMER-80 data have been discussed by Anderson and Dyrssen (1981) and the Hudson-82 data by Chen et al. (1990). The analyses during MIZEX-84 were the same as those used during Hudson-82.

Data to study the input of carbon through the shelf produced high density water were collected in 1983 during the CESAR Ice Camp over the Alpha Ridge and in 1985 during the Lance expedition to the Svalbard region. For more information about the techniques used see Jones and Anderson (1986) and Anderson et al. (1989).

CO_2 ventilation: Deep convection

The CO_2 ventilation through deep convection takes place in the Greenland Sea as the water in the surface mixed layer becomes dense enough through air–sea–ice interactions to sink and form deep water (e.g., Rudels et al., 1989). This means that the deep water formed recently was exposed to an atmosphere with a higher CO_2 partial pressure than that formed 100 years ago. If A_t did not change in the sinking water over the last century, C_t must have increased as the atmospheric CO_2 partial pressure increased (see Fig. 2). The Greenland Sea Deep Water (GSDW) formed by deep convection mixes with the out-flowing Eurasian Basin Deep Water (EBDW) to form the Norwegian Sea Deep Water (NSDW) (see Fig. 5). Some of this NSDW flows back into the Arctic Ocean while some drains over the ridges to form the deep water in the Norwegian Sea. Hence, there are two forms of NSDW, one new (n-NSDW) that is of great importance in the formation of deep water in the Arctic Ocean, and one large pool of water, with quite high mean age, in the Norwegian Sea (o-NSDW) (Swift and Koltermann, 1988). It is the latter one that, together with the intermediate water produced in the Iceland Sea, is involved in the overflow into the North Atlantic Ocean.

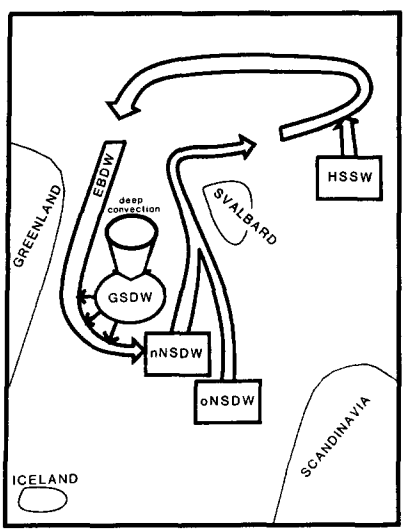

Fig. 5. Schematic scenario of the deep water formation in the Greenland Sea and the mixing regimes in the Fram Strait region of the Arctic Ocean.

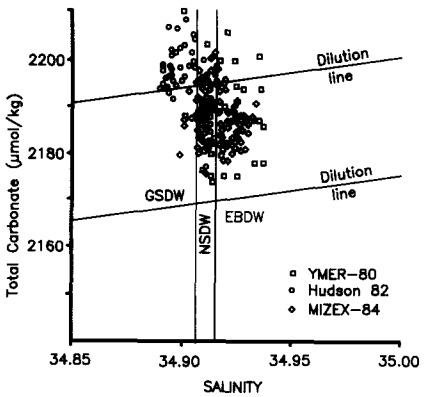

Fig. 6. Total carbonate versus salinity in the deep waters of the Fram Strait region, collected during the YMER-80, Hudson 82 and MIZEX-84 expeditions. The salinity distribution of the water masses, Greenland Sea Deep Water (GSDW), Norwegian Sea Deep Water (NSDW) and Eurasian Basin Deep Water (EBDW), are indicated.

A plot of C_t versus salinity, Fig. 6, illustrates the formation and mixing process described above. The data are all deep samples from the Norwegian Sea, the Greenland Sea and the Fram Strait, collected during the YMER-80, Hudson 82 and MIZEX-84 expeditions. No corrections have been made for decay of organic matter as that would destroy any mixing signatures. The salinity intervals of the water masses are 34.889–34.892 for GSDW, 34.908–34.911 for NSDW and 34.919–34.936 for EBDW (Swift et al., 1983), but as mixing takes place we find a continuous salinity

distribution in the data. Even if though there is much scatter in the data in Fig. 6, some features are quite obvious. (a) GSDW has the highest C_t. This would be even more obvious if the data were corrected for decay of organic matter. This indicates that GSDW is the youngest water and has been in contact with an atmosphere of high pCO_2. (b) The C_t concentrations in the NSDW show the largest concentration interval, a result of the large age distribution. (c) The data are consistent with the mixing regime postulated. The n-NSDW is formed as a result of mixing of GSDW with EBDW and the mean C_t concentration of these waters is in the upper concentration range of that determined for NSDW. (d) EBDW is formed inside the Arctic Ocean when High Salinity Shelf Water (HSSW) is mixed in along the shelf slopes. That the salinity increases is obvious, but no increase of C_t can be seen other than that expected if C_t behaves conservatively, even though the EBDW was formed from the oldest NSDW mixing with High Salinity Shelf Water (HSSW).

It is possible to estimate the input of anthropogenic CO_2 through the deep convection in the Greenland Sea by knowing the volume of water that leaves the surface and by assuming some degree of CO_2 saturation of water (calculated from preformed C_t and A_t). With 100% CO_2 saturation, C_t is 35 μmol/kg higher today with an atmospheric pCO_2 of 350 ppm than in pre-industrial times with an atmospheric pCO_2 of 280 ppm. If a volume of 0.5 Sv leaves the surface (B. Rudels, pers. commun.) the total carbon input is 6×10^{12} g Cy^{-1}. In addition to the deep water formed in the Greenland Sea, water is formed in the Iceland Sea that penetrates to intermediate depths. The volume of this water is in the order of 1 Sv, giving an input of 12×10^{12} g Cy^{-1}.

CO_2 ventilation: Shelf processes

The high density water formed over the shelves transports carbon from the atmosphere to the deep Arctic Ocean through a series of processes. In the summers when the shelves are ice free there is a large biological primary production. This productivity decreases pCO_2 in the surface water, driving the transport of CO_2 from the atmosphere

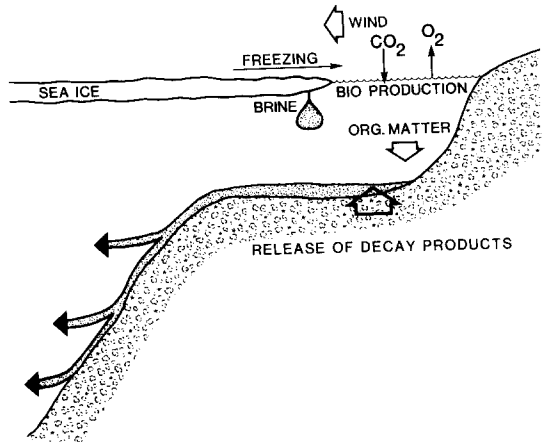

Fig. 7. A schematic illustration of the processes involved in the transfer of chemical constituents from the surface waters over the shelves into the deep basins. (From Anderson and Dyrssen, 1989.)

into the sea. The organic matter dies over the season and most will end up in the surface sediment as the depths are shallow. Here the organic matter decays and the decay products diffuse out into the overlaying water. With the productive season in the summer, there will be maximum organic matter in the sediment in the fall when the ice starts to form. The ice formation produces brine that drains out and forms high density bottom water. The biological decay products, one being C_t, are added to the high density bottom water, which flows out towards the deep interior and interleaves at levels with the appropriate density. A summary of these processes is illustrated in Fig. 7.

The existence of high salinity shelf bottoms water of freezing temperature have been found in the Chukchi Sea by Aagaard et al. (1981) and in the Barents Sea by Midttun (1985). Anderson et al. (1988) report the distribution of some chemical constituents in a pool of high salinity bottom water of freezing temperature in the Storfjorden, Svalbard (Fig. 8). Deeper than about 100 m the water is approximately at the freezing temperature and has a salinity increasing from about 35.2 at 100 m to about 35.5 at the bottom. The distribution with depth for the two deepest stations in the fjord is shown in Fig. 9. There is a significant increase towards the bottom in nutrients and normalized C_t [$C_t(35) = 35C_t/S$)] and a decrease in

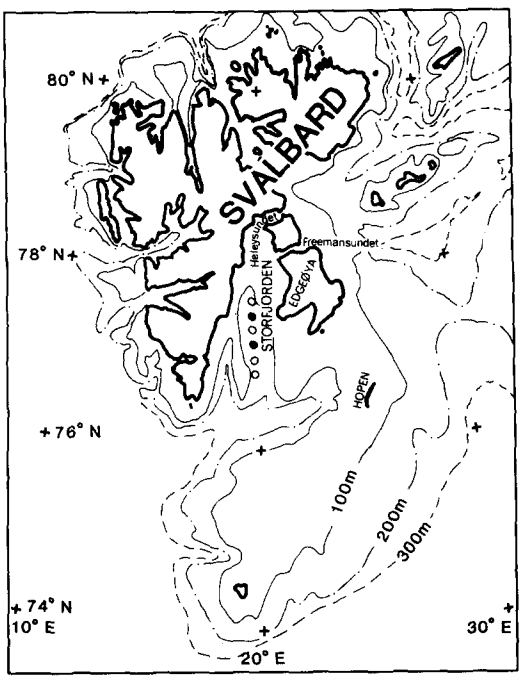

Fig. 8. Map of the Svalbard region with the stations discussed indicated. Filled circles represent the stations shown in Fig. 9. (From Anderson et al., 1988.)

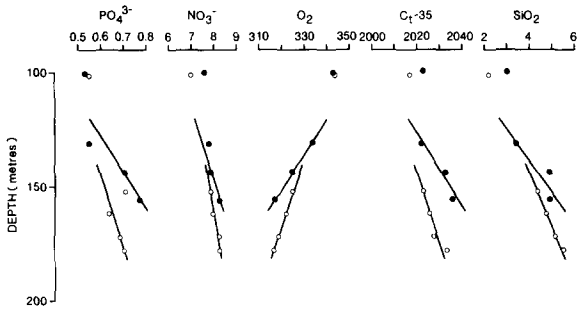

Fig. 9. Nutrients, oxygen and total carbonate in the high salinity bottom waters of the Storfjorden (units are in μmol/kg). Open circles represent the most southern of the two stations indicated in Fig. 8. Lines are fitted to the data points in the water with temperature equal that of freezing at the surface. (From Anderson et al., 1988.)

oxygen, typical signals resulting from the decay of organic matter. The slopes of the concentration gradients should reflect the relative flux of the different constituents from the sediment surface to the bottom water. When the slope is normalized to one phosphate, the result is: 1, 6, 13, −104 and

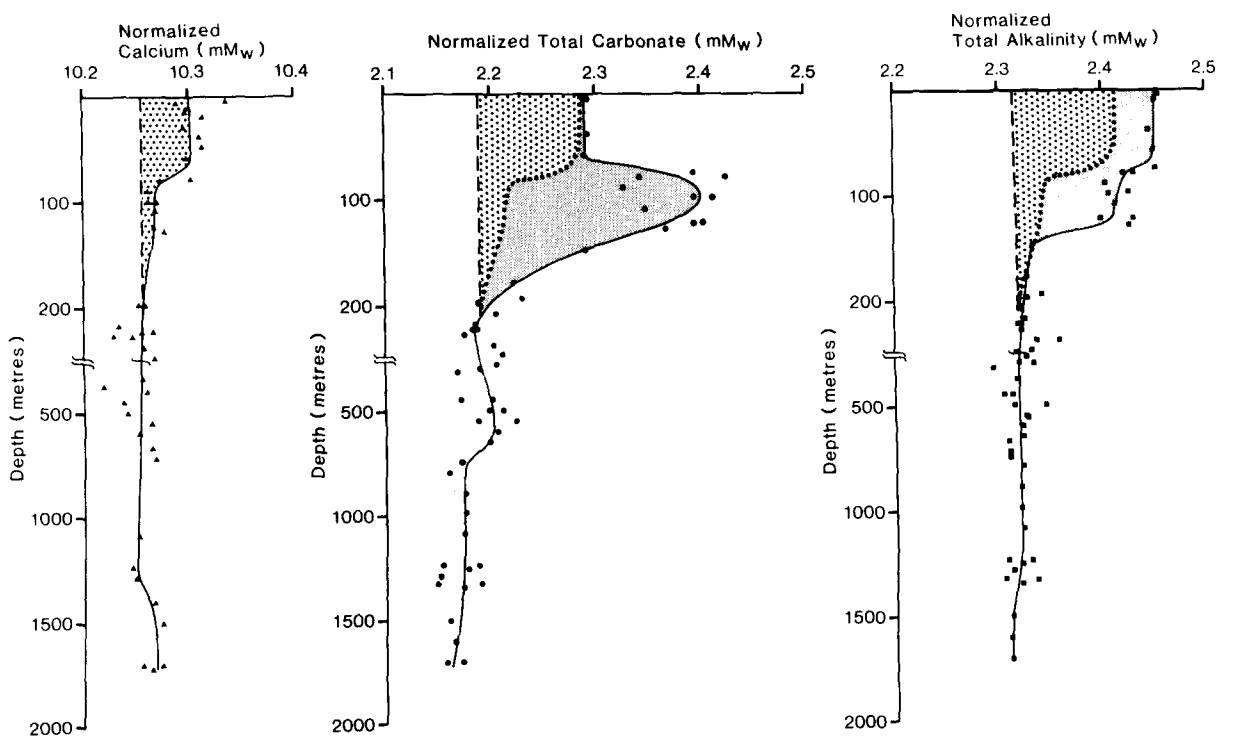

Fig. 10. Total carbonate, total alkalinity and calcium, all normalized to a salinity of 35, in the water column at Ice Station CESAR. The excess total carbonate due to dissolution of calcium carbonate is hatched and the one due to decay of organic matter is dotted. (From Anderson et al., 1990.)

103 for PO_4^{3-}, NO_3^-, SiO_2^-, O_2, and C_t respectively. No depth gradient in A_t could be distinguished. There are two major deviations in the flux from the one expected if the release had followed the classical Redfield et al. (1963) composition of organic matter, the low NO_3^- production and the low O_2 consumption. This can be explained by denitrification, which in itself decreases both the NO_3^- production and the O_2 consumption. It also is an indication of a low oxygen environment, with the result that electron acceptors other than oxygen become involved. However, these different conditions do not change the release of carbon to the high salinity bottom water.

As mentioned above, most of the high salinity shelf water of freezing temperature flows into the upper halocline over the deep basins. In this layer we find a distinct nutrient maximum (Kinney et al., 1970; Moore et al., 1983) which is also complemented by a minimum in oxygen and a maximum in C_t (Jones and Anderson, 1986). The profiles in C_t, A_t and calcium, all normalized to a salinity of 35, at the Ice Camp CESAR (Fig. 10) have been used to estimate the input of carbon to the upper waters of the Arctic Ocean (Anderson et al., 1990). From the distribution of the excess of the different constituents and the known shifts due to the different biochemical reactions (discussed in the Introduction) it is possible to elucidate the origin of the signals. In Fig. 10, the excess due to dissolution of metal carbonate is separated from that of decaying organic matter on the shelves. The dissolution of metal carbonate occurs to a large part in the drainage basins and the excess is transported to the sea by the rivers. The acid consumed during the dissolution is most likely CO_2 from decaying organic matter in the drainage basins.

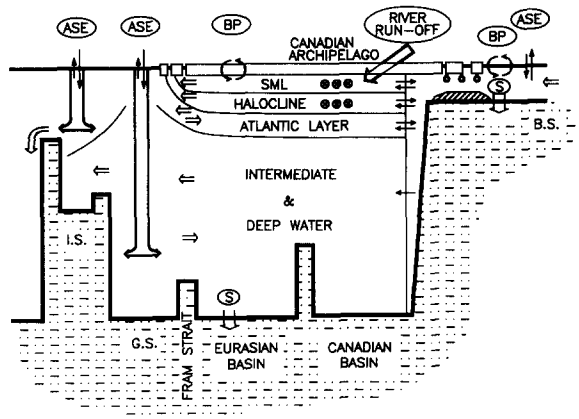

Fig. 11. A schematic illustration of the processes of importance in the transport of carbon in the Arctic Ocean. The processes are Air–Sea Exchange (*ASE*), Biological Production (*BP*), and Sedimentation (*S*), besides the inputs and outputs due to water exchange. For quantitative estimates, see text.

With a knowledge of the areal distribution of the upper layers and the residence times of the different water masses it is possible to estimate the annual net fluxes. This was done by Anderson et al. (1990) and is summarized in Table 1. It should be noted that the fluxes estimated are steady state fluxes and are probably not affected by the atmospheric increase of CO_2, at least not as long as the climate does not change significantly.

A summary of the processes affecting the carbon transport in the Arctic Ocean, including

TABLE 1

Assessment of total carbonate concentration (C_t) and net fluxes into the Arctic Ocean. μM_w denotes micro mol/kg seawater. The residence times are taken from Östlund and Hut (1984) and from Wallace and Moore (1985)

	Res. time (years)	C_t (μM_w)	C_t 1984 (μM_w)	Area (m^2)	Net flux (10^{12} g C yr^{-1})		
					River run off	Shelf	Total
Surface mixed layer	10	2090 ± 9		$8.4 \cdot 10^{12}$	57	0	57
Halocline	10	variable		$5.8 \cdot 10^{12}$	24	96	120
Atlantic layer	30	2176 ± 22	2196	$5.8 \cdot 10^{12}$	0	33	33
Total carbon transport							210
Reference water							
North Atlantic Water in West Spitsbergen Current	0	2160 ± 5	2160				

the Iceland and Greenland Seas, is shown in Fig. 11. Carbon is added through the rivers in the form of HCO_3^- and directly from the atmosphere as CO_2. CO_2 is added mainly over the shelves, where, at least for part of the season, the water is open. The transport between the atmosphere and the sea is driven by CO_2 partial pressure differences at the interface. Partial pressure differences between the atmosphere and the surface water in the Arctic are controlled by three processes: (a) CO_2 is lowered in the surface water by biological primary production, (b) the CO_2 solubility is increased in the surface water when it cools and (c) CO_2 is increasing in the atmosphere.

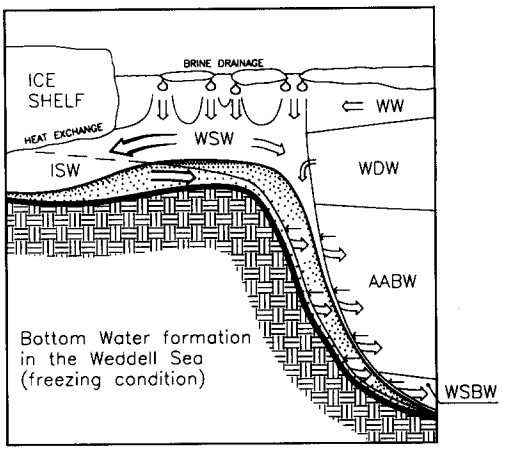

Fig. 12. A simplified illustration of the bottom water formation on the shelves in the southern Weddell Sea. (From Anderson et al., 1991.)

The Weddell Sea

The waters in the Weddell Sea are incorporated into the oceanic system surrounding Antarctica. The Circumpolar Deep Water (CDW), which originates from deep waters of the Atlantic, Pacific and Indian Oceans (Foster and Carmack, 1976), circulate Antarctica from west to east in the circumpolar current. The geographical shape of the Antarctic continent causes a gyre to form in the Weddell Sea where the deep water, the Weddell Deep Water (WDW), is slightly cooler than the CDW. The WDW is formed from CDW to which colder water is added during the circulation in the Weddell Sea. The circulation pattern is such that on the average the WDW circulates several times before a water parcel leaves the gyre and then it leaves in a modified form. Above the WDW is the Winter surface Water (WW) which, during summers, is warmed and has its salinity lowered by sea ice melting. Below the WDW the temperature decreases and we find first the Antarctic Bottom Water (AABW), then, closest to the bottom, the colder Weddell Sea Bottom Water (WSBW).

Deep water formation

Of the seas surrounding Antarctica, the Weddell Sea is perhaps the most important for deep water formation. The deep waters formed around Antarctica have lower salinities and lower temperatures than waters formed in the northern Atlantic Ocean but the resulting density is higher. As a result, it is the AABW that flows over the bottoms of the global oceans

The Antarctic Bottom Water can be formed either by deep convection (probably intermittently) or by shelf processes involving heat exchange with the enormous ice shelves. The latter is a process that has been shown to produce a continuous drain of high density water over the shelf break in the southern Weddell Sea (Foldvik et al., 1985). Figure 12 show a schematic illustration of the formation of high density bottom water on the shelf. As in the Arctic, the process starts with sea ice formation that produces brine, which drains out of the ice and forms high salinity shelf water. The formation of this high salinity shelf water, Western Shelf Water (WSW), occurs mainly in the south western Weddell Sea where it is rather shallow, less than 500 m. The sea ice is formed by freezing of WW and hence any WSW formation results in a inflow of WW to the area. Because of the topography, the WSW flows both to the north, down the shelf slope, and to the south, under the ice shelf. When it flows to the north, it mixes with both WW and WDW to form Weddell Sea Bottom Water (WSBW) (Foster and Carmack, 1976). The WSW that flows to the south exchanges heat at the underside of the ice shelf, leading to a colder but less saline water mass called Ice Shelf Water (ISW). The ISW flows to the north, in topographic canyons, and down the shelf slope,

entraining surrounding water as it goes. Depending on how much of the WDW is entrained, the resulting water is either AABW or WSBW. This mixing pattern can be seen in a temperature–salinity diagram (Fig. 13).

Data

The data to study the input of anthropogenic CO_2 to the deep waters in the Weddell Sea were collected during the Swedish Antarctic Expedition 1988/1989. The analytical procedures used have been discussed by Anderson et al. (1991). The stations sampled were distributed over the Weddell Sea from about 4° W to the peninsula, (see Fig. 18). A plot of the normalized C_t and A_t versus potential temperature for all samples analyzed is shown in Fig. 14.

CO_2 ventilation: Deep convection

There are some indications of deep convection reported in the literature (e.g., Gordon, 1978), but it does not seem to be an annual process as it may be in the Greenland Sea. It is speculated that deep convection occurs during periods when the large polynya is present in the Weddell Sea. It is also believed that deep convection occurs due to topographic conditions, for instance in the Maud Rise area. However, there are no data available, at least to our knowledge, that make it possible to estimate the ventilation of CO_2 in the Antarctic due to deep convection.

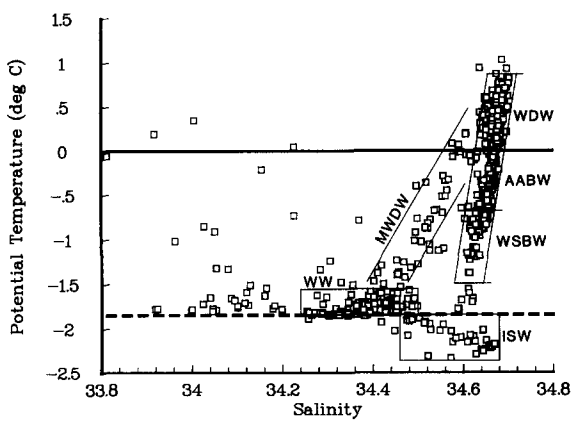

Fig. 13. Potential temperature versus salinity for the bottle data collected during the Swedish Antarctic Expedition 1988/1989 (SWEDARP 88/89). The different water masses are illustrated.

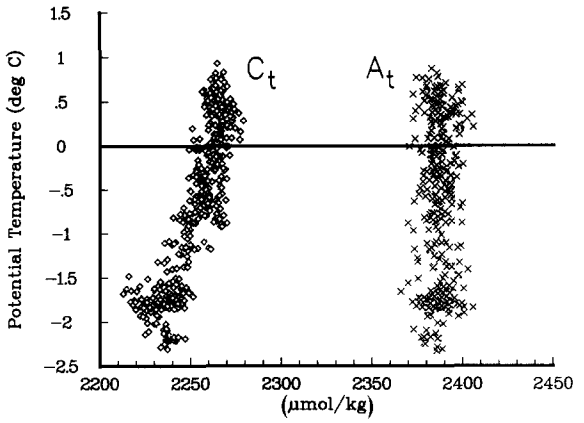

Fig. 14. Potential temperature versus total carbonate (diamonds) and total alkalinity (crosses), normalized to a salinity of 35, for all samples analyzed during SWEDARP 88/89. (From Anderson et al., 1991.)

CO_2 ventilation: Shelf processes

The flux of CO_2 into the surface waters of the Weddell Sea has been changing over approximately the last 150 years because of the increasing atmospheric CO_2 partial pressure. The increase in pCO_2 results in an increased concentration of C_t (Fig. 2). In order to evaluate this increase we have to correct C_t for changes resulting from the decay of organic matter and the dissolution of metal carbonate. The A_t concentrations (Fig. 14) indicate that dissolution of metal carbonate can be neglected. This is in accordance with other investigations (e.g., Poisson and Chen, 1987). The correction due to decay of organic matter can be done using the apparent oxygen utilization (AOU) and the ratio of carbon to oxygen in organic matter. Using the ratio reported by Redfield et al. (1963) we get the following equation,

$$C_t\text{-corr} = C_t\text{-meas} - 106/138\text{AOU} \quad (1)$$

where C_t-meas is the measured total carbonate concentration. A plot of C_t-corr (normalized to $S = 35$) versus potential temperature is shown in Fig. 15. There is a significantly larger scatter in the shallow data, mainly as a result of primary production and the escape of oxygen to the atmosphere in the surface water at the time of the

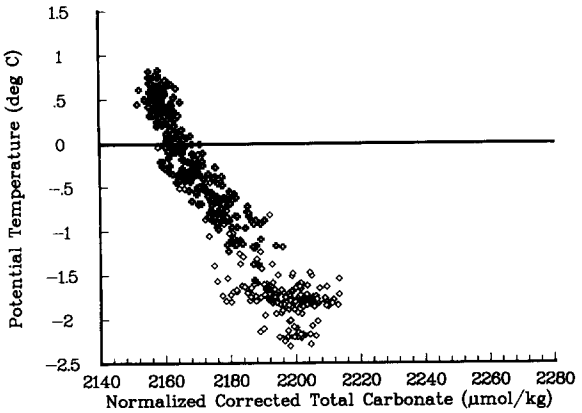

Fig. 15. Potential temperature versus total carbonate corrected for decay of organic matter, assuming the Redfield et al. (1963) ratios of organic matter and 100% oxygen saturation. The corrected data have been normalized to a salinity of 35. The crosses represent samples deeper than the temperature maximum while the diamonds represent shallower samples.

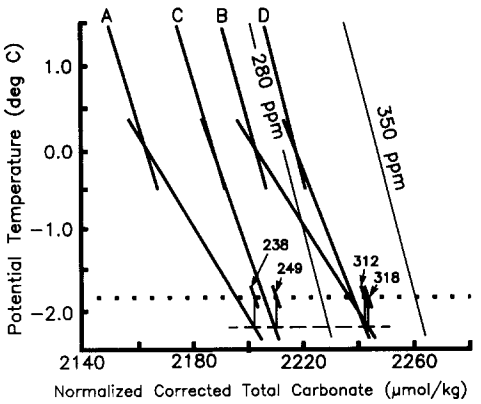

Fig. 16. Lines fitted to the data of normalized corrected total carbonate, where the corrections have been done assuming the following ratios of C_t to O_2 in organic matter and degrees of oxygen saturation: *A*, 106 to 138 and 100% O_2-sat. *B*, 106 to 138 and 86% O_2-sat. *C*, 103 to 176 and 100% O_2-sat. *D*, 103 to 176 and 86% O_2-sat. (From Anderson et al., 1991.)

investigation. Nevertheless, it is obvious that the ISW (Theta $< -2°$C) mixes with the water close to zero degrees (also seen in Fig. 14 for the uncorrected C_t). This is what normally is set as the lower temperature limit of the WDW. The data with temperatures above zero degrees are associated with a line of different slope than that of the mixing line between ISW and WDW at zero degrees, a slope that is close to the one for a given pCO_2 in Fig. 2.

The correction for decay of organic matter according to eqn. (1) assumes 100% oxygen saturation when the water left the surface. The measured oxygen saturation in the WW during the winter is reported to be 86%. (Gordon et al., 1984). Also the Redfield et al. (1963) ratio of carbon to oxygen is questionable (see the Introduction). Plots of potential temperature vs. normalized C_t-corr for 100% and 86: oxygen saturation with the Redfield et al. (1963) and the Takahashi et al. (1985) ratios are given in Fig. 16, with lines fitted to the data. The degree of CO_2 saturation of the ISW when it left the surface (as WSW) is calculated by taking the C_t value at the ISW temperature (about $-2.2°$C), moving this to the temperature of freezing (assuming that the only change was in temperature and not in C_t) at one atmosphere pressure and fitting it to an atmospheric pCO_2 (as illustrated in Fig. 2). As the water sank very close to the time when it was sampled, 350 ppm is used as reference to calculate the percentage saturation. Table 2 summarizes the calculations for the different scenarios. It is seen that by using the measured oxygen saturation, 86%, the CO_2 saturation is

TABLE 2

Equilibrium concentrations of CO_2 (ppm) and degrees of saturation in the Sink Water assuming different relations of carbon and oxygen in organic matter and different degrees of oxygen saturation. *A* to *D* denotes the scenarios in Fig. 16. Sink Water represents the ISW when it left the surface

Assumptions				Sink Water	
del O_2	del C_t	O_2-sat		pCO_2-eq (ppm)	CO_2-sat (rel. 350 ppm)
−135	106	100	*A*	238	68
−135	106	86	*B*	318	91
−172	103	100	*C*	249	71
−172	103	86	*D*	312	89

close to 90% with both the Redfield et al. (1963) and the Takahashi et al. (1985) carbon to oxygen ratios for the organic matter. Hence, this ratio is not considered to be critical for the evaluation of the CO_2 input.

In pre-industrial times the atmospheric pCO_2 was around 280 ppm. The WDW, as described above, is an old water that left the surface well before industrialization started and thus has not been significantly affected by increased atmospheric pCO_2 as seen in the ^{14}C signal (Weiss et al., 1979). It is presumed that when the ISW was formed before industrialization it had the same degree of CO_2 saturation as now. This would give a mixing line for the ISW with WDW at zero degrees shown by the dotted line of Fig. 17. The difference between the continuous and dotted line in Fig. 17 should then reflect the anthropogenic input. The concentration varies with temperature which of course is due to the mixing of waters with high (ISW) and very low (WDW) anthropogenic CO_2 concentrations.

By taking the difference between the dotted line of Fig. 17 and the normalized corrected measured C_t data, we get the anthropogenic CO_2 in each sample. A plot of these for different sections

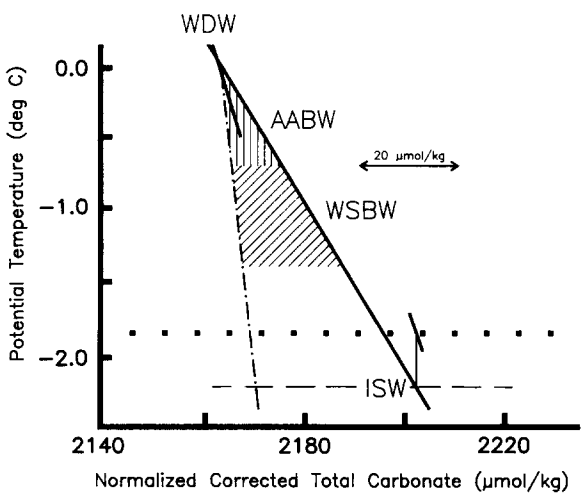

Fig. 17. The mixing line for scenario A of Fig. 16, solid line, and the corresponding line (dotted) but with the assumption that the ISW left the surface when the atmospheric pCO_2 was 280 ppm (preindustrial time). The difference between the lines equals the anthropogenic CO_2 concentration in the different water masses.

across the shelf slope shows the penetration of anthropogenic CO_2 in the Weddell Sea (Fig. 18). It is clear that the most easterly section has very little anthropogenic CO_2 in the deep waters, while there must be an inflow east of the one at about 36° W. (Remember that there is a clockwise gyre in the Weddell Sea.) This inflow is coming from the Filchner Depression which has been shown to be a significant drainage area of ISW (Foldvik et al., 1985).

Current meter observations at the shelf break just west of the Filchner Depression gave a mean flow of 0.7 Sv at −2° C (Foldvik et al., 1985). At this temperature the mean anthropogenic CO_2 concentration is 29 μmol kg^{-1} (Fig. 17) which results in an annual transport of 8×10^{12} g C. The anthropogenic CO_2 pattern in the sections suggests that there are areas of significant deep water penetration between the section at 40° W and the one at the peninsula. However, it is unlikely that they will transport more than two times what is transported out through the Filchner Depression (also indicated by the estimates by Carmack and Foster, 1975), making the total annual input to the Weddell Sea not more than 25×10^{12} g C.

Summary and conclusions

The inputs of CO_2 to the Arctic Ocean can be divided into one steady state input and one anthropogenic. The annual steady state input is 210×10^{12} g C, while the anthropogenic is $12 \pm 6 \times 10^{12}$ g C considering the deep convection in both the Greenland and Iceland Seas, estimated to 1 ± 0.5 Sv (B. Rudels, pers. commun.).

For the Weddell Sea area we do not have an estimate of the annual steady state input, but it should be significant because of the relatively large biological production. The annual anthropogenic input is calculated to be 8×10^{12} g C draining out through the Filchner Depression. We also estimate the maximum input through other deep water formation areas on the shelves in the Weddell Sea to be 16×10^{12} g C annually. These rather low estimates of anthropogenic CO_2 input are in agreement with the concentrations found in the Atlantic and Southern oceans by Chen (1982).

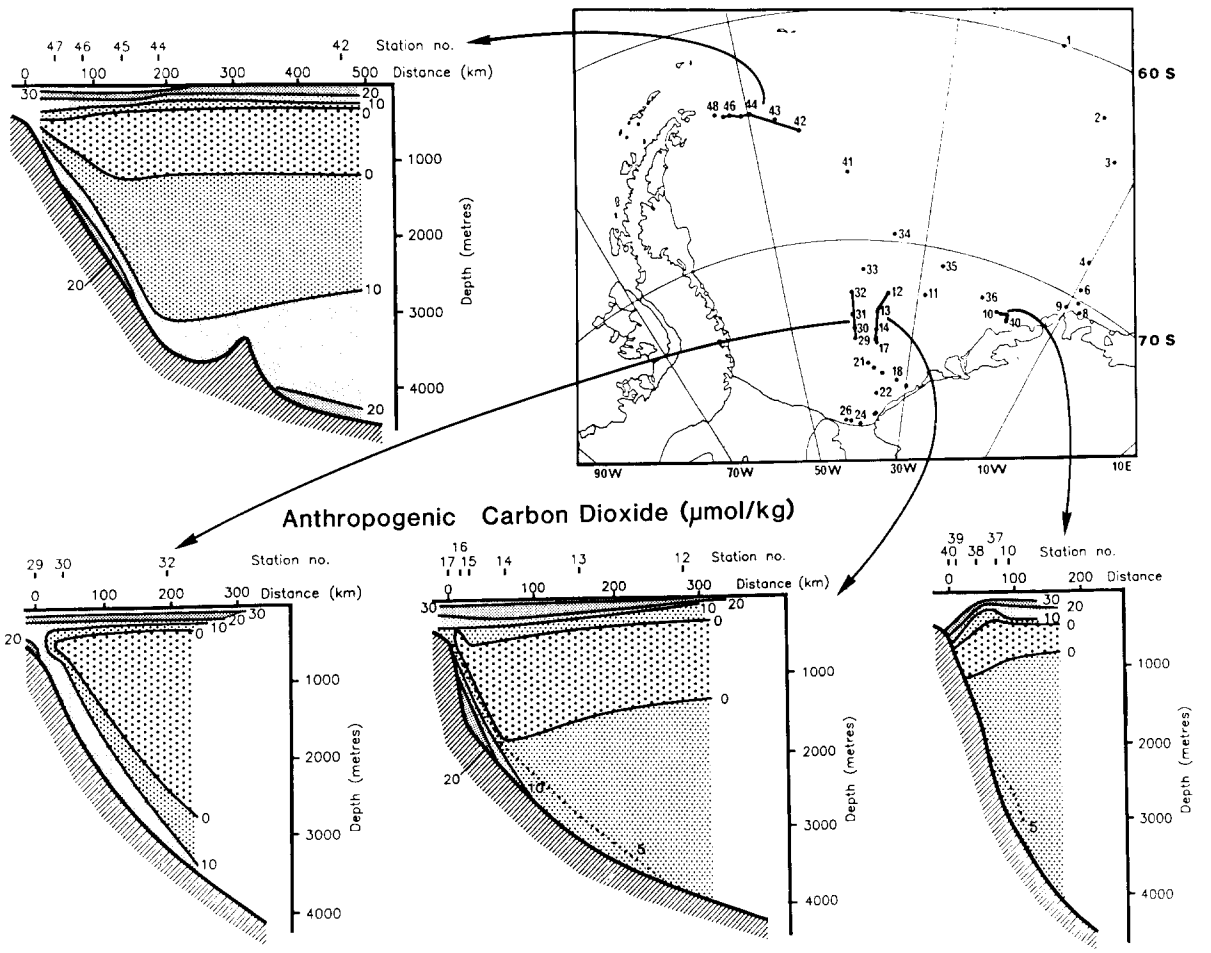

Fig. 18. The anthropogenic CO_2 concentration along the shelf slopes at different locations in the Weddell Sea (calculated as the difference between the corrected measured data and the dotted line of Fig. 17).

In the Arctic Ocean, shelf processes dominate the steady input of CO_2 while in the Weddell Sea they provide an anthropogenic input. Deep convection in both polar regions causes an input of anthropogenic CO_2, the magnitude in the Antarctica is, however, uncertain due to a lack of data.

The annual anthropogenic CO_2 sink is in the order of $12 \pm 6 \times 10^{12}$ g C in the Arctic Ocean including the GIN Seas and maximum 24×10^{12} g C in the Weddell Sea. Even with other ventilation areas of the same order in Antarctica, the total annual input will most likely not exceed 50×10^{12} g C. These ventilation rates should be compared to the annual anthropogenic emission, about 5500 $\times 10^{12}$ g C. Hence, it is concluded that the polar oceans are not a significant sink of anthropogenic CO_2. However, this does not necessarily mean that the polar oceans are not important in the global change perspective, as they are very sensitive to changes in the climate which might very well significantly change their ability to sequester CO_2, especially that due to biological production (e.g., Walsh, 1989).

Acknowledgment

We are grateful to the Department of Fisheries and Oceans, Canada, the Alfred Wegener Institute of Polar and Marine Research, Germany and the Swedish Polar Research Secretariat who gave us the opportunity to take part in the YMER-80, Hudson-82, MIZEX-84 and SWEDARP 88/89 expeditions on which the data discussed in this

paper were collected. Financial support from the Swedish Natural Science Research Council, Knut and Alice Wallenberg Foundation, Marianne and Marcus Wallenberg Foundation, Erna and Victor Hasselblad Foundation and Sven and Dagmar Salén Foundation is also gratefully acknowledged.

References

Aagaard, K., Coachman, L.K. and Carmack, E.C., 1981. On the halocline of the Arctic Ocean. Deep-Sea Res., 28: 529–545.

Aagaard, K., Swift, J.H. and Carmack, E.C., 1985. Thermohaline circulation in the Arctic mediterranean seas. J. Geophys. Res., 90: 4833–4946.

Aagaard, K. and Carmack, E.C., 1989. The role of sea ice and other fresh water in the Arctic circulation. J. Geophys. Res., 94: 14485–14498.

Anderson, L. and Dyrssen, D., 1981. Chemical constituents in the Arctic Ocean in the Svalbard area. Oceanol. Acta, 4: 305–311.

Anderson, L.G., Jones, E.P., Lindegren, R., Rudels, B. and Sehlstedt, P.-I., 1988. Nutrient regeneration in cold, high salinity bottom water of the Arctic shelves. Cont. Shelf-Res., 8:1345–1355.

Anderson L. and Dyrssen, D., 1989. Chemical oceanography of the Arctic Ocean. In: Y. Herman (Editor), The Arctic Seas; Climatology, Oceanography, Geology, and Biology. van Nostrand Reinhold Company, New York. pp. 93–114.

Anderson, L.G., Dyrssen, D. and Jones, E.P., 1990. An assessment of the transport of atmospheric CO_2 into the Arctic Ocean. J. Geophys. Res., 95: 1703–1711.

Anderson, L.G., Holby, O., Lindegren, R. and Ohlson, M., 1991. The transport of anthropogenic carbon dioxide into the Weddell Sea. submitted to J. Geophys. Res.

Björk, G., 1989. A one-dimensional time-dependent model for the vertical stratification of the upper Arctic Ocean. J. Phys. Oceanogr., 19: 52–67.

Carmack, E.C. and Foster, T.D., 1975. On the flow of water out of the Weddell Sea Deep-Sea Res., 22: 711–724.

Chen, C.-T.A., 1982. On the distribution of anthropogenic CO_2 in the Atlantic and Southern oceans. Deep-Sea Res., 29: 563–580.

Chen, C.-T.A., Jones, E.P. and Lin, K., 1990. Wintertime anthropogenic carbon dioxide measurements in the northern North Atlantic Ocean. Deep-Sea Res., 37: 1455–1473.

Dyrssen, D., 1977. The chemistry of plankton production and decomposition in seawater. In: N.R. Andersen and B.J. Zahuranec (Editors), Oceanic Sound Scattering Prediction. pp 65–84, Plenum Press.

Dyrssen, D. and Wedborg, M., 1982 The influence of the partial pressure of carbon dioxide on the total carbonate of seawater. Mar. Chem., 11: 183–185.

Foldvik, A., Gammelröd, T. and Törresen, T., 1985. Physical oceanography studies in the Weddell Sea during the Norwegian Antarctic Research Expedition 1987/79. Polar Res., 3: 195–207.

Foster, D.F. and Carmack, E.C., 1976. Frontal zone mixing and Antarctic Bottom Water formation in the southern Weddell Sea. Deep-Sea Res., 23: 301–317.

Gordon, A.L., 1978. Deep Antarctic convection west of Maud Rise. J. Phys. Oceanogr., 8: 600–612.

Gordon, A.L., Chen, C.-T.A. and Metcalf, W.G., 1984. Winter mixed layer entrainment of Weddell Deep Water. J. Geophys. Res., 89: 637–640.

Jones, E.P. and Anderson, L.G. 1986., On the origin of the chemical properties of the Arctic Ocean halocline. J. Geophys. Res., 91: 10759–10767.

Kinney, P., Arhelger, M.E. and Burrell, D.C., 1970. Chemical characteristics of water masses in the Amerasian Basin of the Arctic Ocean. J. Geophys. Res., 75: 4097–4104.

Melling, H. and Lewis, E.L., 1982. Shelf drainage flows in the Beaufort Sea and their effect on the Arctic Ocean pycnocline. Deep-Sea Res., 29: 967–985.

Midttun, L., 1985 Formation of dense bottom water in the Barents Sea. Deep-Sea Res., 32: 1233–1241.

Moore, R.M., Lowings, M.G. and Tan, F.C., 1983 Geochemical profiles in the central Arctic Ocean: Their relation to freezing and shallow circulation, J. Geophys. Res., 88: 2667–2674.

Östlund, H.G. and Hut, G., 1984. Arctic Ocean water mass balance from isotope data. J. Geophys. Res., 89: 6373–6381.

Poisson, A. and Chen, C.-T.A., 1987. Why is there little anthropogenic CO_2 in the Antarctic Bottom Water? Deep-Sea Res., 34: 1255–1275.

Quadfasel, D., Rudels, B. and Kurz, K., 1988. Outflow of dense water from a Svalbard fjord into the Fram Strait. Deep-Sea Res., 35: 1143–1150.

Redfield, A.C., Ketchum, B.H. and Richards, F.A., 1963. The influence of organisms on the composition of sea water. In: M.N. Hill (Editor) The Sea, vol. 2. Interscience, New York, pp. 26–77.

Rudels, B., 1986. The Θ-S relations in the Northern Seas: Implications for the deep circulation. Polar Res., 4: 133–159.

Rudels, B., Quadfasel, D. Friedrich, H. and Houssais, M.-N, 1989. Greenland Sea convection in the winter of 1987-1988. J. Geophys. Res., 94: 3223–3227.

Smethie, Jr, W.M., Chipman, D.W. Swift, J.H. and Koltermann, K.P., 1988 Chlorofluoromethanes in the Arctic mediterranean seas: Evidence for formation of bottom water in the Eurasian Basin and deep-water exchange through Fram Strait. Deep-Sea Res., 35: 347–369.

Subba Rao, D.V. and Platt, T., 1984. Primary production of arctic waters. Polar Biol., 3: 191–201.

Swift, J.H., Takahashi, T. and Livingston, H.D., 1983. The contribution of Greenland and Barents Seas to the Deep Water of the Arctic Ocean. J. Geophys. Res., 88: 5981–5986.

Swift, J.H. and Koltermann, K.P., 1988. The origin of Norwegian Sea Deep Water. J. Geophys. Res., 93: 3563–3569.

Takahashi, T., Broecker, W.S. and Langer, S., 1985. Redfield ratios based on chemical data from isopycnal surfaces. J. Geophys. Res., 90: 6907–6924.

Wallace, D.W.R. and Moore, R.M., 1985. Vertical profiles of CCl3F (F-11) and CCl2F2 (F-12) in the central Arctic Ocean basin. J. Geophys. Res., 90: 1155–1166.

Wallace, D.W.R., Moore, R.M. and Jones, E.P., 1987. Ventilation of the Arctic Ocean cold halocline: Rates of diapycnal and isopycnal transport, oxygen utilization and primary production inferred using chlorofluoromethane distributions. Deep-Sea Res., 34: 1957–1979.

Walsh, J.J., 1989. Arctic Carbon Sinks: Present and Future. Global Biogeochem. Cycles, 3: 393–411.

Weiss, R.F., 1974. Carbon dioxide in water and seawater: The solubility of a non-ideal gas. Mar. Chem., 2: 203–215.

Weiss, R.F., Östlund, H.G. and Craig, H., 1979. Geochemical studies of the Weddell Sea. Deep-Sea Res., 26: 1093–1120.